Journal of Molecular Catalysis A: Chemical 304 (2009) 8–15

Contents lists available at ScienceDirect

Journal of Molecular Catalysis A: Chemical

journal homepage: www.elsevier.com/locate/molcata

Pd^{II} square planar complexes of the type $[IL]_2[PdX_4]$ as catalyst precursors for the Suzuki–Miyaura cross-coupling reaction. The first *in situ* ESI-MS evidence of $[(IL)_xPd_3]$ clusters formation

W. Zawartka [a], A. Gniewek [a], A.M. Trzeciak [a,*], J.J. Ziółkowski [a], J. Pernak [b]

[a] *Faculty of Chemistry, University of Wrocław, 14 F. Joliot-Curie, 50-383 Wrocław, Poland*
[b] *Poznań University of Technology, pl. M. Skłodowskiej-Curie 2, 60-965 Poznań, Poland*

ARTICLE INFO

Article history:
Received 4 October 2008
Received in revised form 8 January 2009
Accepted 9 January 2009
Available online 20 January 2009

Keywords:
Palladium complexes
N-Heterocyclic carbenes
Palladium nanoparticles
ESI-MS
Suzuki–Miyaura

ABSTRACT

Pd^{II} anionic, square planar complexes of the type $[IL]_2[PdX_4]$, where IL = imidazolium cations, X = Cl, Br, have been applied for the first time as catalyst precursors for the Suzuki–Miyaura (S–M) reaction carried out in alcohols at 40 °C. Depending on the structure of the catalyst precursor used, different yields of 2-methylbiphenyl (2-MePh–Ph) were obtained in a test reaction of 2-bromotoluene (2-MePhBr) with phenyl boronic acid ($PhB(OH)_2$). The highest yield, *ca.* 95%, was obtained for $[dmiop]_2[PdCl_4]$ (dmiop-1,2-dimethyl-3-propoxymethylene imidazolium cation) in methanol in the presence of KOH as a base. It was found that during the reaction Pd^0 nanoparticles of 4–7 nm have been formed *in situ* from the palladium(II) precursor. In the first stage of this process, $[(IL)_3Pd(OH)_2]^+$-type species have been formed from $[IL]_2[PdX_4]$ precursors. Small Pd^0 clusters, $[(IL)_5Pd_3(H_2O)]^+$ and $[(IL)_3Pd_3(H_2O)_7]^+$, were also identified by ESI-MS. These species reacted with $ArB(OH)_2$ forming palladium aryl complexes of the type $[(IL)_2PdAr]^+$, key intermediates in the catalytic process. The first experimental evidence of the IL stabilized Pd^0 species in S–M reaction is presented.

1. Introduction

Complexes of the type $[IL]_2[PdX_4]$ have never been used before as catalyst precursors for the Suzuki–Miyaura (S–M) reaction, and also there are only scarce examples of their successful application in other catalytic processes. One of the first papers describes synthesis, structure, and application of $[bmim]_2[PdCl_4]$ as a selective although not very active catalyst for hydrodimerization of 1,3-butadiene [1]. The same complex has been used as a catalyst for the oxidation of alcohols: 3-Me-cyclohexanol, isophorol, geraniol, and $Me(CH_2)_{17}OH$ [2]. The formation of $[Bu_4N]_2[PdX_4]$-type complexes has been observed in the Heck reaction when $PdCl_2$, $PdCl_2(PhCN)_2$, and $Pd(OAc)_2$ complexes were used as catalyst precursors in molten tetrabutylammonium bromide as the reaction medium [3,4]. The same complexes have been formed as a result of leaching when Pd^0 supported on alumina was used as a catalyst for the Heck reaction carried out in a $[Bu_4N]Br$ medium [4].

The synthesis, structure, and stability of $[IL]_2[PdX_4]$-type complexes (where IL = imidazolium or pyridinium cation, X = Cl, Br) have been discussed in several papers [1–10]. Complexes containing imidazolium cations with long-chain alkyl (R) substituents (C_{12}, C_{18}) demonstrate properties of liquid crystals with crystallite sizes of around 2 Å [1].

Recently we have applied $[IL]_2[PdX_4]$ complexes as catalyst precursors for methoxycarbonylation of iodobenzene in ionic liquids [10]. Yields of up to 100% were obtained when the reaction was carried out in pyridinium salts, whereas imidazolium halides surprisingly inhibited the reaction. This inhibiting effect, causing a very low yield of the methoxycarbonylation product, was explained by the reaction of imidazolium halide with an intermediate aryl complex, [Ar–Pd(II)-X], formed by oxidative addition of aryl halide (ArX) to the Pd^0 active species. The reaction of the palladium aryl complex with imidazolium halide finally led to the formation of a carbene compound of the type $PdCl_2(bmim\text{-}y)_2$, less active in methoxycarbonylation [10].

Motivated by these interesting results obtained with the application of $[IL]_2[PdX_4]$-type complexes as catalyst precursors for methoxycarbonylation, we decided to check their catalytic properties also in the S–M reaction. In these studies we were looking for a correlation between the structure of the imidazolium cation (IL^+) and the catalytic activity of palladium(II) square planar complexes of the type $[IL]_2[PdX_4]$. Identification of catalytically active

* Corresponding author. Tel.: +48 71 3757 253; fax: +48 71 3757 356.
E-mail address: ania@wchuwr.pl (A.M. Trzeciak).

1381-1169/$ – see front matter © 2009 Elsevier B.V. All rights reserved.
doi:10.1016/j.molcata.2009.01.011

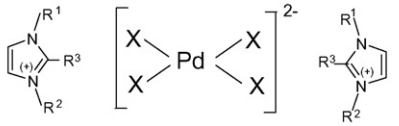

IL	$[emim]^+$	$[bmim]^+$	$[miop]^+$	$[mioe]^+$	$[bdmim]^+$	$[dmiop]^+$
R^1	C_2H_5	C_4H_9	$CH_2OC_3H_7$	$CH_2OC_2H_5$	C_4H_9	$CH_2OC_3H_7$
R^2	CH_3	CH_3	CH_3	CH_3	CH_3	CH_3
R^3	H	H	H	H	CH_3	CH_3

Fig. 1. $[IL]_2[PdX_4]$ complexes under studies as Pd-catalyst precursors (X = Cl, Br).

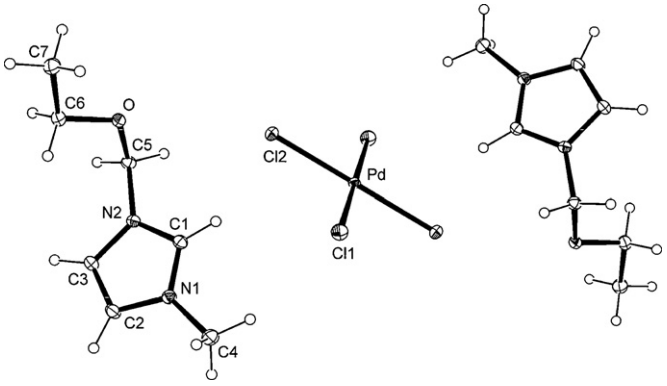

Fig. 2. The molecular structure and atom numbering scheme of $[mioe]_2[PdCl_4]$. Displacement ellipsoids are drawn at the 30% probability level and H atoms are shown as small spheres of arbitrary radii. Unlabeled atoms are symmetrically dependent via an inversion center. Pd–Cl1 2.314 (8); Pd–Cl2 2.303 (8); O–C5 1.389 (2); O–C6 1.436 (2); Cl1–Pd–Cl2 89.50 (3) C5–O–C6 113.4 (2); Cl1–Pd–Cl2# 90.50 (3); #symmetry transformations used to generate equivalent atoms: # $1-x$, $1-y$, $1-z$. Hydrogen bonding parameters are given in Table 7.

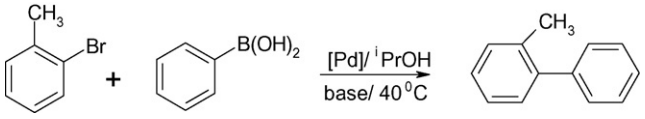

Fig. 3. The S–M reaction under studies.

intermediates and mechanistic aspects were the main objective of the presented studies.

2. Results and discussion

2.1. Effect of the IL^+ cation in $[IL]_2[PdX_4]$ complexes on their activity as catalyst precursors

Palladium(II) complexes of the general formula $[IL]_2[PdX_4]$, shown in Fig. 1, with different substituents, R^1 and R^2, in the imidazolium cations and Cl or Br ions coordinated to Pd^{II}, were used as catalyst precursors.

The molecular structure of $[mioe]_2[PdCl_4]$, presented as an example in Fig. 2, shows square planar coordination of chlorides and symmetrical arrangement of imidazolium cations. The planes of the imidazolium rings are parallel to each other.

Five different complexes of the type $[IL]_2[PdX_4]$ were tested as catalyst precursors for the S–M reaction at 40 °C in 2-propanol (Fig. 3, Table 1).

It was found that the kind of imidazolium cation present in the precursor has an essential influence on the S–M reaction yield. The highest yields of the product (2-MePh–Ph), 84% and 83%, were obtained for $[dmiop]_2[PdCl_4]$ and $[bdmim]_2[PdBr_4]$, respectively.

Table 1
The yield of 2-MePh–Ph obtained in the S–M reaction with different catalyst precursors (Fig. 1) after 1, 2, 3, and 4 h.

Catalyst precursor	Yield[a] (%)			
	1 h	2 h	3 h	4 h
$[bmim]_2[PdCl_4]$	34	39	52	
$[bdmim]_2[PdBr_4]$	44	54	58	
$[dmiop]_2[PdCl_4]$	35	63	70	84
$[mioe]_2[PdCl_4]$	8	33	36	
$[Bu_4N]_2[PdBr_4]$			68	82

Reaction conditions: [Pd] 1×10^{-5} mol; 2-MePhBr 1×10^{-3} mol; $PhB(OH)_2$ 1.1×10^{-3} mol; KOH 1.95×10^{-3} mol; 2-propanol 3 cm^3; 40 °C.
[a] The reaction yield is equivalent to TON.

We found these results very interesting because both cations having a Me group at carbon C2 (C2—carbon atom between two nitrogen atoms in imidazolium cation) are unable to form carbene ligands, which makes it possible to rule out the formation of carbene complexes as catalytically active species in this S–M reaction. On the other hand the high catalytic activity of palladium complexes with bulky carbene ligands in the S–M reaction is well documented in literature [11–14].

The higher product yield obtained with palladium precursor ($[dmiop]_2[PdCl_4]$) containing ether functional group imidazolium cation can be explained by the stabilizing effect of ether moiety on the palladium active form, as it was recently proposed [15].

Lower S–M reaction yields were obtained for complexes containing a 1-butyl-3-methyl imidazolium cation (bmim) (52%) or a 1-butyl-2,3-dimethyl imidazolium cation (bdmim) (58%). For the complex with a 1-methyl-3-ethoxymetyl imidazolium cation (mioe), only 36% of the product was obtained. In all S–M reactions, besides 2-MePh–Ph, the main product, only traces, up to 3%, of biphenyl (Ph–Ph), the homocoupling product, were found.

S–M reactions were also performed with the $PdCl_2$(cod) precursor with the addition of stoichiometric amounts of ionic liquids ([IL]X) in methanol solution. When only the $PdCl_2$(cod) complex was used as a catalyst precursor, 25% of 2-MePh–Ph was obtained. The addition of ionic liquids ([IL]X) in the amount of [[IL]X]/[Pd] = 2:1 was expected to lead to *in situ* formation of $[IL]_2[PdX_4]$ complexes, identical to those previously used as catalyst precursors. However, the yields of S–M reactions in most cases appeared much lower compared with those obtained for ready

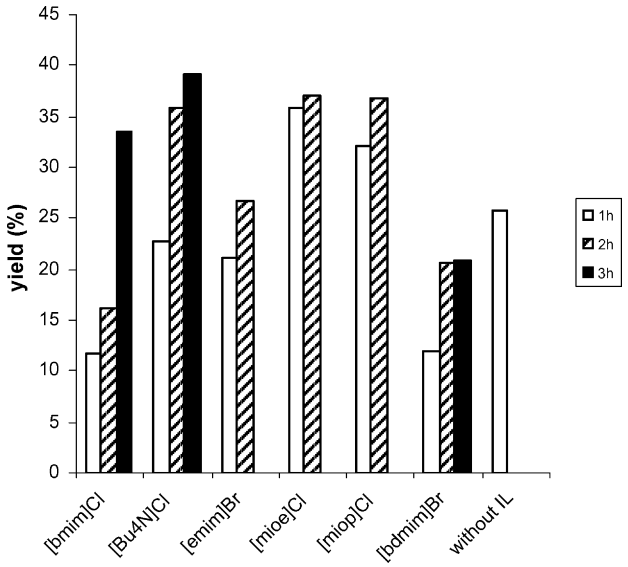

Fig. 4. The yield of 2-MePh–Ph obtained in the S–M reaction with $PdCl_2$(cod) and different ionic liquids in methanol ([IL]: [Pd] = 2), after 2 h at 40 °C.

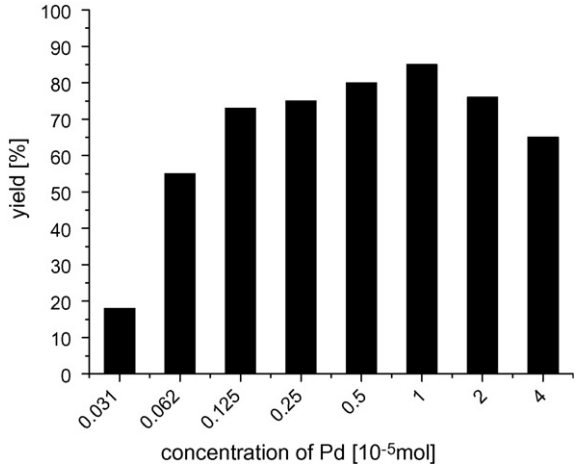

Fig. 5. Effect of $[dmiop]_2[PdCl_4]$.concentration on the S–M reaction yield. $PhBrCH_3$ 1×10^{-3} mol; $PhB(OH)_2$ 1.1×10^{-3}mol; KOH 1.95×10^{-3}mol; 2-propanol, 3 h, 40 °C.

precursors of the type $[IL]_2[PdX_4]$. Only the addition of [miop]Cl or [mioe]Cl caused an increase in the coupling product yield in comparison to the reaction without an ionic liquid (Fig. 4). The maximum yield of the S–M reaction for such systems, after 2 h, was 37%.

The addition of an ionic liquid ([IL]X) to the best precursor, $[dmiop]_2[PdCl_4]$, caused a decrease in 2-MePh–Ph yield to below 70% after 3 h. In the presence of different [IL]X the following yields of 2-MePh–Ph were obtained: 68% for [dmiop]Cl, 38% for $[bmim]BF_4$, and 44% for [bmim]Br.

2.2. Effect of catalyst precursor concentration, kind of base and solvent used on the S–M reaction yield

The effect of the concentration of $[dmiop]_2[PdCl_4]$ on the reaction yield is shown in Fig. 5.

The highest yield, 84% (TOF = 28 h^{-1}), was obtained for 1×10^{-5} mol, whereas at lower and higher concentrations of the catalyst precursor the obtained yields were lower (Fig. 5). At a concentration as low as 3.12×10^{-7} mol, 18% (TOF = 193 h^{-1}) of the product was still obtained after 4 h. The highest TOF value, 296 h^{-1}, was found for 6.2×10^{-7} mol (yield 55%). The nonlinear dependence of the S–M reaction yield on the concentration of the catalyst precursor may suggest contribution of Pd^0 nanoparticles as reactive species in this reaction. Such conclusion has been formulated for the Heck reaction catalyzed by $Pd(OAc)_2$ [16].

Table 2
The yield of 2-MePh–Ph obtained in the S–M reaction with $[dmiop]_2[PdCl_4]$ as the catalyst precursor in different solvents and bases after 1, 2, 3, and 4 h.

Solvent	Yield[a] (%)				
	Base	1 h	2 h	3 h	4 h
Methanol	KOH	86	90	89	95
2-Propanol	KOH	35	63	70	84
	NaOH	29	29	65	
	K_3PO_4	36	61	63	
	NaOAc	4	5	8	
	KOAc	12	21	35	
	$NaHCO_3$	1	3	3	
	NaO^tBu	18	27	28	
Pentanol	KOH	68	63	63	
2-Butanol	KOH	58	–	61	
Water	KOH	13	14	23	

Reaction conditions: [Pd] 1×10^{-5} mol; 2-MePhBr 1×10^{-3} mol; $PhB(OH)_2$ 1.1×10^{-3} mol; base 1.95×10^{-3} mol; solvent 3 ml; 40 °C.
[a] see Table 1.

Table 3
UV–vis spectra (nm) of $[IL]_2[PdX_4]$ complexes before and after reduction with KOH/2-propanol.

$[IL]_2[PdX_4]$	Before the reduction λ_{max} (nm)		After the reduction λ_{max} (nm)
$[bmim]_2[PdCl_4]$	326	250	240
$[bdmim]_2[PdBr_4]$	286	220	222
$[dmiop]_2[PdCl_4]$	326	250	242; 290 sh
$[mioe]_2[PdCl_4]$	330	248	220–230 br., 280 sh
$[emim]_2[PdBr_4]$	286	218	220–240 br.; 285 sh

The effect of the kind of base and solvent on the S–M reaction yield is illustrated by the data collected in Table 2.

The best results were obtained with KOH, whereas a lower yield of 2-MePh–Ph was obtained with NaOH. A similar effect has been explained by other authors as resulting from the different reactivity of the respective propanolates formed *in situ* when the reaction is carried out in 2-propanol [17,18]. However, the application of sodium *t*-butanolate gave only 28% of 2-MePh–Ph, indicating a more complex relationship. It can be suggested that a positive role is played by the bigger size of the alkaline cation (K^+ versus Na^+), and in fact an unexpectedly good result (63% yield) was obtained with K_3PO_4. The effect of the solvent was also found important (Table 2), and generally alcohols were found to be better solvents than water. The best result (95% of 2-MePh–Ph) was obtained for a reaction carried out in methanol, and the second best (84%) for 2-propanol. For butanol and pentanol the yields obtained after 3 h were 61% and 63% respectively, whereas for water the yield was only 23%. The effect of the solvent can be related to the rate of $Pd^{II} \rightarrow Pd^0$ reduction and deactivation of the system by the formation of palladium black when reduction is too fast. This explanation is supported by the spontaneous formation of palladium black in reactions carried out in water.

2.3. Reduction of Pd^{II} to colloidal Pd^0 nanoparticles

In all the S–M reactions under study, with different Pd-catalyst precursors and various basic solutions of alcohols as reaction media, colloidal nanoparticles of Pd^0 were formed. Their formation was first signalized by the change of the brown-red colour of Pd^{II} solution to almost black at the end of reaction. As a consequence, UV–vis spectra changed and the bands at 284–330 nm assigned for Pd^{II} square planar complexes disappeared, and only UV-bands were observed (Table 3).

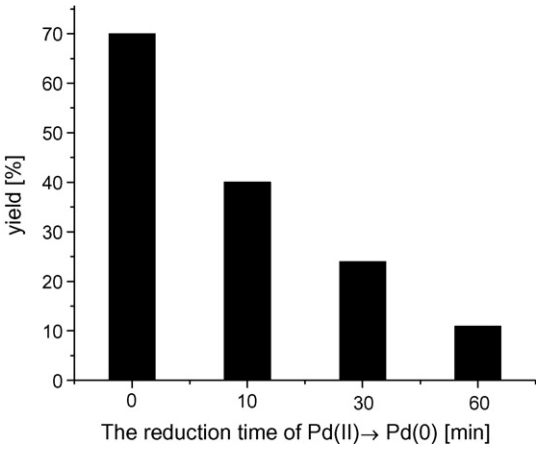

Fig. 6. The yield of 2-MePh–Ph in the S–M reaction catalyzed with Pd^0 nanoparticles obtained by reduction of $[dmiop]_2[PdCl_4]$ with KOH/2-propanol over different lengths of time.

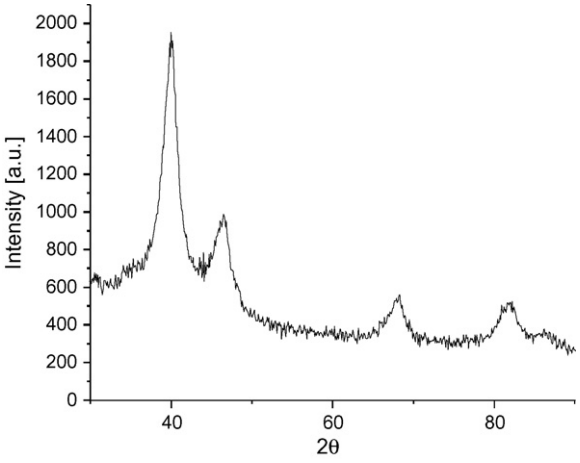

Fig. 7. The XRD pattern of Pd^0 nanoparticles obtained by the reduction of $[bmim]_2[PdBr_4]$ with KOH/2-propanol at 80 °C, 1 h.

The influence of the $Pd^{II} \rightarrow Pd^0$ reduction rate on catalytic activity was tested using the $[dmiop]_2[PdCl_4]$ complex as the catalyst precursor. The reaction mixture containing this precursor and KOH in 2-propanol was stirred for a certain time, and next the substrates (2-MePhBr and $PhB(OH)_2$) were added. From the results presented in Fig. 6, one may conclude that the extension of the palladium pre-treatment time led to significant deactivation of the catalyst demonstrated by a decrease in the yield of the product.

Fig. 7 presents the XRD pattern of the sample obtained in a 1 h reaction of $[bmim]_2[PdBr_4]$ with KOH/2-propanol, confirming the complete reduction of Pd^{II} to Pd^0. The XRD measurements allowed us to determine the presence of Pd^0 nanoparticles and their size (from the line broadening measured at $2\theta = 40.1^\circ$). The average size of Pd^0 nanoparticles obtained from the $[dmiop]_2[PdCl_4]$ precursor after 10 min reaction time with KOH/2-propanol was *ca.* 4 nm. When the reduction time was prolonged to 30 min, the size of obtained particles increased to 7.3 nm. One may conclude that elongation of the reduction time lead to the formation of bigger particles and, as a consequence, less active (Fig. 6).

Table 4
ESI-MS(−) and ESI-MS(+) data of $[IL]_2[PdX_4]$ complexes.

Complex	ESI-MS(−); *m/z*				ESI-MS(+); *m/z*	
$[bmim]_2[PdCl_4]$	177.8	$[PdCl_2]^-$	212.8	$[PdCl_3]^-$	139.1	$[bmim]^+$
$[bdmim]_2[PdBr_4]$	266.7	$[PdBr_2]^-$	346.7	$[PdBr_3]^-$	153.1	$[bdmim]^+$
$[dmiop]_2[PdCl_4]$	177.8	$[PdCl_2]^-$	212.8	$[PdCl_3]^-$	169.1	$[dmiop]^+$
$[mioe]_2[PdCl_4]$	177.8	$[PdCl_2]^-$	212.8	$[PdCl_3]^-$	141.1	$[mioe]^+$
$[emim]_2[PdBr_4]$	266.7	$[PdBr_2]^-$	346.7	$[PdBr_3]^-$	111.1	$[emim]^+$

2.4. ESI-MS studies of palladium intermediates formed in the S–M reaction: detection of IL stabilized Pd^0 particles

The formation of Pd^0 nanoparticles in S–M reaction is well documented in the literature [19–22] however very little is known about the mechanism of this process. We chosen the ESI-MS method [23–26] for identification of palladium intermediates in S–M reaction.

The ESI-MS spectra of $[IL]_2[PdX_4]$ complexes showed the presence of $[IL]^+$ cations and PdX_2 and PdX_3 anions (Table 4).

As expected, palladium was present only in anions, which was evidenced by the characteristic isotopic distribution pattern of *m/z* signals assigned to PdX_2^- and PdX_3^-. PdX_3^- anionic species can be easily formed after X^- dissociation from the parent anion PdX_4^{2-}, whereas PdX_2 is probably present in its neutral form and undergoes

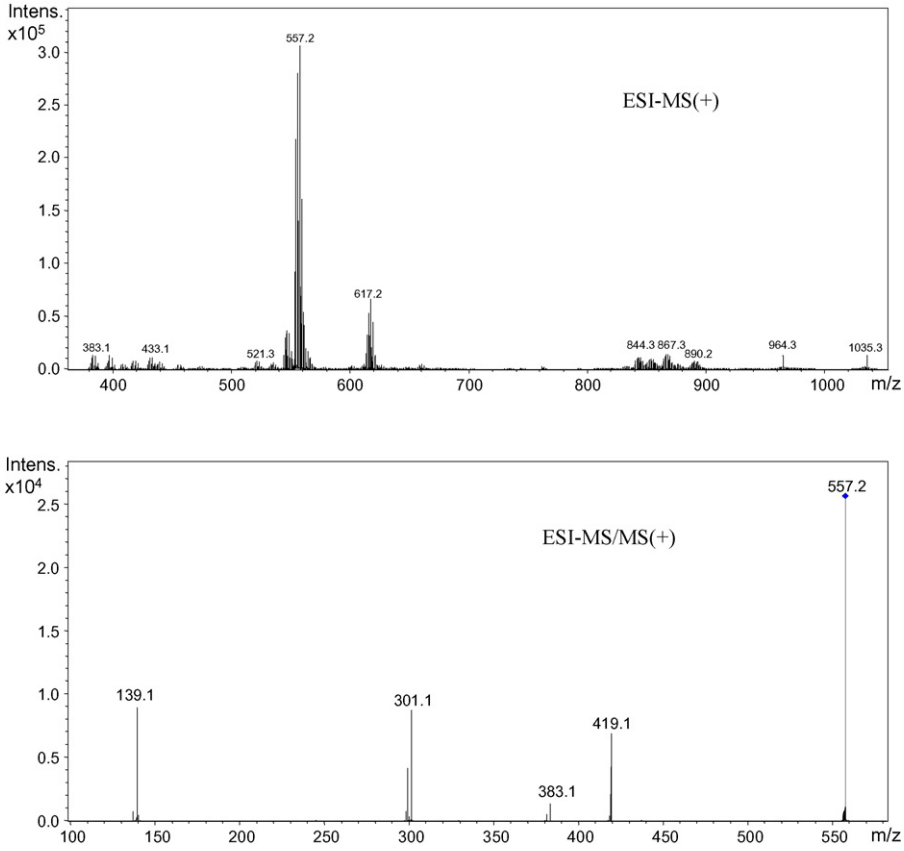

Fig. 8. ESI-MS(+) of $[bmim]_2[PdCl_4]$ after 30 min reaction with KOH/2-propanol (upper) and ESI-MS/MS(+) of the signal at *m/z* 557.2 (lower).

Table 5
ESI-MS(+) and ESI-MS/MS(+) data of Pd^0 species obtained in reactions $[IL]_2[PdX_4]$ + KOH/2-propanol and $[bmim]_2[PdX_4]$ + KOH/2-propanol + $ArB(OH)_2$ (Ar = C_6H_5, $CH_2=CHC_6H_4$).

Complex $[IL]_2[PdX_4]$	ESI-MS(+); m/z $[IL]_2[PdX_4]$ + KOH/2-propanol
$[bmim]_2[PdCl_4]$	383.1; 419.1; 433.1; 467.1; 487.1; 546.2; 557.2*[a]; 581.2; 617.2; 761.2; 842.3; 867.3; 955.4; 988.1; 1038
$[bdmim]_2[PdBr_4]$	557.1; 681.4[b]
$[dmiop]_2[PdCl_4]$	681.4[c]
$[mioe]_2[PdCl_4]$	387.1; 412.1; 423.1; 432.1; 512.0; 552.2; 568.2*[a]; 656.2; 815.6
$[emim]_2[PdBr_4]$	325.1; 352.1; 363.0; 407.0; 417.0; 431.1; 446.1; 473.1*[a]; 462.2*[d]; 517.1; 549.2; 666.6; 743.1; 750.1
[a] $[(IL)_3Pd(OH)_2]$; [b] $[(IL)_3PdBr(OH)(H_2O)]^+$; [c] $[(IL)_3PdCl_2]^+$; [d] $[(IL)_3Pd(OH)]^+$	
*ESI(+)-MS/MS	
557.2 → 419.1 → 383.1 → 301.1 → 139.1	
568.2 → 430.1 → 387.1	
473.1 → 363.1 → 327.1	
462.2 → 351.6 → 329.1 → 136.1 → 111.1	
$[bmim]_2[PdCl_4]$ + KOH/2-propanol + $ArB(OH)_2$	
Ar: C_6H_5	459.2; 524.1; 597.3*[e]
Ar: $CH_2=CHC_6H_4$	383.1; 485.2; 623.3*[e]
[e] $[(bmim)_3\ PdAr]^+$	
*ESI(+)-MS/MS	
597.3 → 459.2 → 215.2	
623.3 → 485.2 → 381.1 → 241.2 → 139.1	

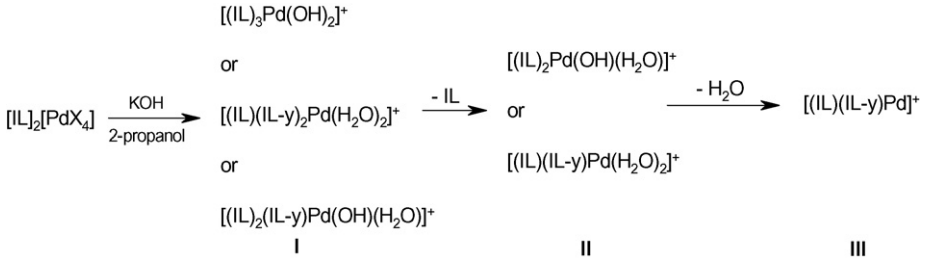

Fig. 9. Fragmentation pattern of the product of $[IL]_2[PdX_4]$ reduction with KOH/2-propanol.

ionization during the ESI process [27]. It can also be supposed that the PdX_2^- anion contains Pd^I formed by reduction of Pd^{II} with X^-.

Analysis of spectra registered for samples obtained from the reaction of $[IL]_2[PdX_4]$ complexes with KOH in 2-propanol disclosed the presence of totally new signals (Fig. 8).

The most interesting and characteristic observation was that palladium was found exclusively in cationic forms (ESI(+)), and not in anionic ones (PdX_2^-, PdX_3^-) found in the starting complexes.

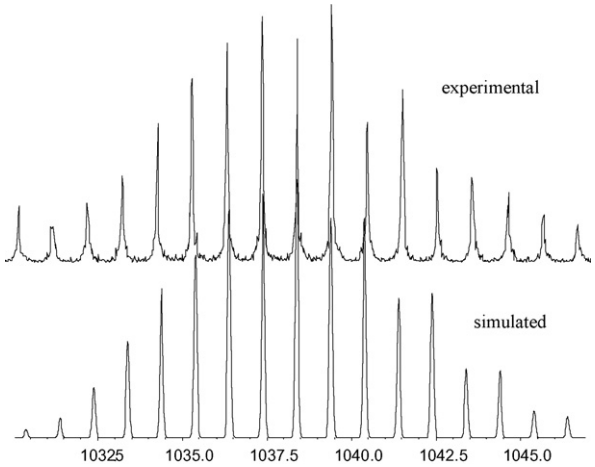

Fig. 10. Experimental (upper) and simulated (lower) fragment of MS spectrum of $[(bmim)_5Pd_3(H_2O)]^+$ (or $[(bmim)(bmim\text{-}y)_4Pd_3(H_2O)]^+$.

For further studies, we selected the ESI-MS(+) spectra of products derived from $[IL]_2[PdX_4]$ complexes containing different $[IL]^+$ cations (IL = bmim, mioe, emim), for which the most abundant signals were those at m/z = 557, 563, and 471 respectively. Analysis of ^{106}Pd isotopologue by the ESI-MS/MS(+) method made it possible to establish the composition of the first intermediate products as $[(IL)_3Pd(OH)_2]^+$ (Table 5).

In addition, reduction of $[bmim]_2[PdCl_4]$ with NaOH/2-propanol instead of KOH/2-propanol produced the same forms of palladium, which warrants the conclusion that neither K^+ nor Na^+ is present in the detected cationic fragments. The presence of halide ions in the main reduction products was also ruled out because identical spectra were obtained for both palladium precursors, $[bmim]_2[PdCl_4]$ and $[bmim]_2[PdBr_4]$.

It is worth noting that only in two cases, for $[dmiop]_2[PdCl_4]$ and $[bdmim]_2[PdBr_4]$ reduced with KOH/2-propanol, the most abundant cations observed in MS spectra contained halide ions. The

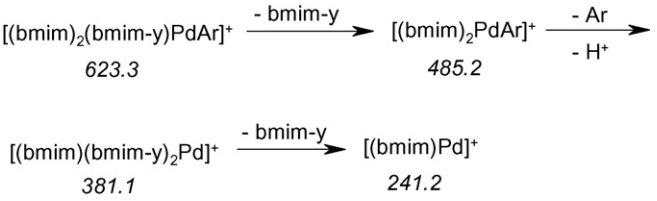

Fig. 11. Fragmentation pattern of the reaction product of $[bmim]_2[PdCl_4]$ with $(CH_2=CHPh)B(OH)_2$ in a KOH/2-propanol medium.

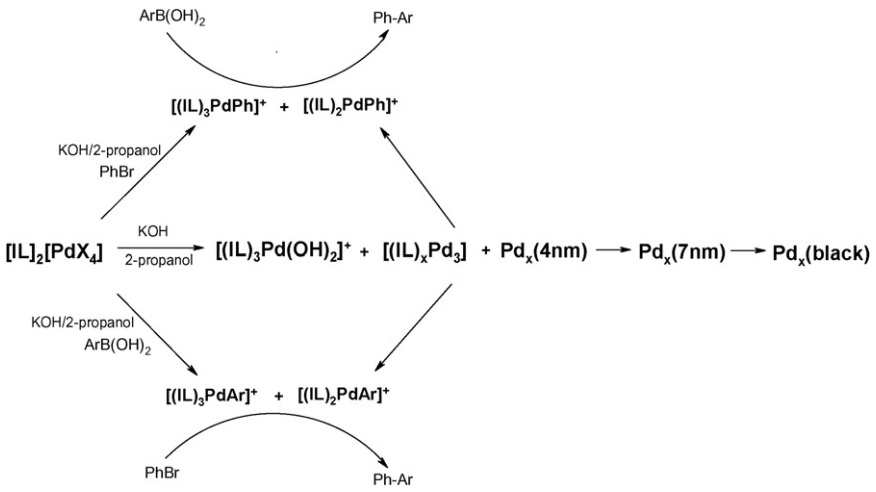

Fig. 12. Transformations of $[IL]_2[PdX_4]$ precursors under the S–M reaction conditions.

signal at $m/z = 681.4$ originating from $[dmiop]_2[PdCl_4]$ was assigned to $[(dmiop)_3PdCl_2]^+$, whereas for $[bdmim]_2[PdBr_4]$, the signal at $m/z = 681.4$ was assigned to $[(bdmim)_3PdBr(OH)(H_2O)]^+$. Thus, under the same reaction conditions, halide-containing species are more stable when imidazolium cation bonded to Pd^0 is substituted at C2 by a methyl group.

For complete interpretation of the obtained results, two alternative forms of cationic species $[(IL)_3Pd(OH)_2]^+$ (Fig. 9, I) should be also considered: $[(IL)(IL\text{-}y)_2Pd(H_2O)_2]^+$ and $[(IL)_2(IL\text{-}y)Pd(OH)(H_2O)]^+$, where IL-y = *N*-heterocyclic carbene formed by abstraction of H^+ from C2 of imidazolium cation.

Fig. 9 presents the general scheme of the fragmentation of $[(IL)_3Pd(OH)_2]^+$ cations under ESI-MS/MS(+) conditions. What is crucial is that in the first step one (IL^+) cation is lost. The other (IL^+) or (IL-y) ligands are bonded to palladium more strongly, and they are present even in the third (last) fragment ($[(IL)(Il\text{-}y)Pd]^+$) (Fig. 9, III).

Table 6
Crystal data and structure refinement for $[mioe]_2[PdCl_4]$.

Formula	$C_{14}H_{26}Cl_4N_4O_2Pd$
M_r	530.58
Crystal system	Monoclinic
Space group	$P2_1/n$
a/Å	9.442(2)
b/Å	11.244(3)
c/Å	10.155(3)
α/°	90
β/°	94.19(3)
γ/°	90
V/Å^3	1075.2(5)
Z	2
D_c/g cm^{-3}	1.639
μ/mm^{-1}	1.38
T/K	100(2)
Color	Brown
Crystal size/mm	0.34 × 0.24 × 0.16
Absorption correction	Analytical
T_{min}/T_{max}	0.764/0.888
Measured reflections	10410
Unique reflections	2461
Reflections with $I > 2\sigma(I)$	2076
R_{int}	0.038
θ range/°	3.5–27.5
Data/restraints/parameters	2461/0/117
Goodness of fit on F^2	1.01
$R1$, $wR2$ $[I > 2\sigma(I)]$	0.023, 0.049
$R1$, $wR2$ (all data)	0.032, 0.051
Max/min residual density/e Å^{-3}	0.88/−0.38

In the MS spectra of the products obtained in reaction of $[bmim]_2[PdCl_4]$ with a KOH/2-propanol mixture, a number of signals in the range between $m/z = 844$ and 1035 were observed in addition to $[(bmim)_3Pd(OH)_2]^+$ ($m/z = 557.2$) (Fig. 8). Their isotopic distribution pattern indicated the presence of three palladium atoms forming $[(IL)_xPd_3]$ clusters, as confirmed by MS spectrum simulation. Fig. 10 presents a fragment of the ESI(+)-MS spectrum at $m/z = 1035$ and its simulation as $[(bmim)_5Pd_3(H_2O)]^+$ or, with agreement with a +1 charge, $[(bmim)(bmim\text{-}y)_4Pd_3(H_2O)]^+$.

The formation of polymetallic fragments, stabilized with imidazolium cations (IL^+) or with *N*-heterocyclic carbenes (IL-y) maybe considered as the initial stage of $[Pd^0]_x$ nanoparticle formation. Analysis of the ESI-MS(+) spectrum in the region of $m/z = 842$–890 performed by means of simulation indicates that the best agreement can be obtained for $[(bmim)_3Pd_3(H_2O)_x]^+$ or $[(bmim)_4Pd_3(H_2O)_x]^+$. Similarly to the case of the $m/z = 1035$ ion, one can propose that some imidazolium cations (bmim) are present in their deprotonated form as *N*-heterocyclic carbenes (bmim-y) to explain the +1 charge of detected ions.

Studying ESI-MS spectra after different reaction times, we observed that the signals of monomeric forms appeared at the beginning of the reaction and then disappeared. Polynuclear fragments can be observed after 10 min, are well detected after 30 min, and their concentration increases until 1 h. After a longer reaction time those polymetallic species disappeared totally.

Further ESI-MS studies concerned the identification of important intermediates in the S–M reaction. In reaction of $[bmim]_2[PdCl_4]$ with $PhB(OH)_2$ in a KOH/2-propanol medium, the cationic species $\{[bmim]_3PdPh\}^+$, with $m/z = 597$, was identified. When $PhB(OH)_2$ was replaced by $CH_2 = CHPhB(OH)_2$, the corresponding cation $\{[bmim]_3Pd(CH_2 = CHPh)\}^+$, with $m/z = 623$,

Table 7
Hydrogen bonding geometry (Å, °) in compound $[mioe]_2[PdCl_4]$.

D–H···A interaction	D–H	H···A	D···A	D–H···A
C1–H1···Cl1	0.95	2.86	3.685 (3)	145
C1–H1···Cl2	0.95	2.81	3.540 (3)	135
C2–H2···Cl2$^{\#1}$	0.95	2.74	3.555 (3)	144
C3–H3···Cl1$^{\#2}$	0.95	2.85	3.781 (3)	166
C4–H4B···Cl1	0.98	2.91	3.829 (3)	157
C5–H5B···Cl2	0.99	2.63	3.442 (3)	139
C5–H5A···Cl2$^{\#3}$	0.99	2.75	3.552 (3)	139
C7–H7A···O$^{\#4}$	0.98	2.64	3.450 (3)	140

Symmetry transformations used to generate equivalent atoms. #1: $-0.5 + x$, $1.5 - y$, $0.5 + z$; #2: $-0.5 + x$, $1.5 - y$, $-0.5 + z$; #3: $0.5 - x$, $0.5 + y$, $0.5 - z$; #4: x, $-1 + y$, z.

was recorded (Table 5). In this way the presence of one aryl fragment in each $\{[bmim]_3Pd\text{-}Ar\}^+$ species was confirmed. A better formula describing this species, consistent with the +1 charge, is $[(bmim)_2(bmim\text{-}y)PdAr]^+$. The application of the ESI(+)-MS/MS method for fragments with $m/z = 597$ and $m/z = 623$ indicated dissociation of cations with $m/z = 138$ or $m/z = 139$, corresponding to [bmim-y] in the first step. The finally formed ion with $m/z = 241$ corresponds to $[Pd(bmim)]^+$, indicating strong interaction of Pd^0 with the imidazolium cation (Table 5, Fig. 11).

It is worth noting that identical ions containing aryl ligand ($[(bmim)_2(bmim\text{-}y)PdAr]^+$) were also identified in the reaction mixture containing $PhB(OH)_2$ and 2-MePhBr.

3. Conclusions

It was demonstrated that $[IL]_2[PdX_4]$ complexes exhibit good catalytic activity in the S–M reaction already at 40 °C. Under the reaction conditions, Pd^{II} is reduced to Pd^0. In the first step, in the presence of KOH/2-propanol, monomolecular cationic species of the type $[(IL)_3Pd(OH)_2]^+$ are formed, next trimeric clusters of $[(IL)_xPd_3]$ type, and finally $[Pd^0]_x$ nanoparticles of 4–7 nm in size (Fig. 12). In all these forms, imidazolium cations or *N*-heterocyclic carbenes are present and probably act as stabilizing agents preventing fast palladium agglomeration to "palladium black". According to the ESI(+)-MS results, it should be concluded that IL^+ transforms easily to IL-y and *vice versa*. As a result, palladium complexes with *N*-heterocyclic carbenes can participate in the catalytic process with $[IL]_2[PdX_4]$ precursors. The most important for the S–M reaction are monomolecular species, small clusters, and nanoparticles (4–7 nm). Agglomeration of palladium nanoparticles led to an increase in their size and a simultaneous decrease in their the catalytic activity.

4. Experimental

4.1. Preparation of $[bdmim]_2[PdBr_4]$ (bdmim-1-butyl-2,3-dimethyl imidazolium cation)

0.153 g (0.70 mmol) of [bdmim]Br was added to the solution of 0.1 g (0.35 mmol) $PdCl_2(cod)$ [28] in hot CH_3CN (5 cm^3). The mixture was heated for 15 min, until the yellow solution became red. After cooling down the product was precipitated by addition of toluene (1 cm^3). Product yield: 95%.

Elemental analysis: calc (%). for $PdC_{18}H_{36}Br_4N_4$: C 29.4, H 4.9, N 7.6; found: C 28.8, H 4.9, N 7.5. ^{1}H NMR (300 MHz, CD_3CN, 25 °C, TMS): $\delta = 7.33$ (s, 2H, –CH=CH–), 4.1 (t, J(H,H) = 7 Hz, 2H; N–CH_2–), 3.7 (s, 3H, N–CH_3), 2.5 (s, 3H, C–CH_3), 1.7 (qi, J(H,H) = 8 Hz, 2H, –CH_2–), 1.33 (sx, J(H,H) = 8 Hz, 2H, –CH_2–), 0.93 ppm (t, J(H,H) = 8 Hz, 3H, –CH_3).

^{13}C NMR (75.5 MHz, CD_3CN, 25 °C): $\delta = 153.7$ (–N–CH–N–), 123.2; 121,8 (–CH=CH–), 48.9 (N–CH_2), 36(–CH_2–), 32 (N–CH_3), 20; 13.7 (–CH_2–), 10.3 ppm (CH_2–CH_3).

4.2. Preparation of $[mioe]_2[PdCl_4]$ (mioe-1-methyl-3-ethoxymethylene imidazolium cation)

0.115 g (0.70 mmol) of [mioe]Cl was added to the solution of 0.1 g (0.35 mmol) $PdCl_2(cod)$ [28] in hot CH_3CN (5 cm^3). The mixture was heated for 15 min, until the yellow solution became orange. After cooling down the product was precipitated by addition of diethyl ether (3 cm^3). Product yield: 90%.

Elemental analysis: calc (%). for $PdC_{14}H_{28}N_4O_2Cl_4$: C 31.6, H 5.3, N 10.5; found: C 32.0, H 5.5, N 10.8.

^{1}H NMR (300 MHz, CD_3CN, 25 °C, TMS): $\delta = 9.6$ (s, 3H, N–CH–N), 7.6; 7.5 (d, J(H,H) = 2 Hz, 2H, –CH=CH–), 5.6 (s, 2H, –CH_2–O–), 3.9 (s, 3H, =N–CH_3), 3.6 (m, J(H,H) = 7 Hz, 2H, –CH_2–), 1.14 ppm (t, J(H,H) = 7 Hz, 3H, –CH_3).

^{13}C NMR (75.5 MHz, CD_3CN, 25 °C): $\delta = 138.4$ (–N–CH–N–), 124.9; 122.3(–CH=CH–), 79.5 (–N–CH_2–O–), 71.9(s, –N–CH_3), 66.4 (–O–CH_2–CH_3), 37.1 (–N–CH_3), 15 ppm (–CH_2–CH_3).

4.3. Preparation of samples for XRD measurements

After the S–M reaction, the product and the organic substrates were extracted with 10 cm^3 of *n*-hexane. Boric compounds were removed by washing of the residue with 10 cm^3 of water. The black powder was drained under vacuum.

Pd^0 nanoparticles were characterized by a signal (1 1 1) at $2\theta = 40.1°$.

4.4. Preparation of samples for ESI-MS measurements

0.02 g NaOH (or KOH) in 2-propanol (3 cm^3) was stirred in a Schlenk tube for 10 min at 40 °C. Next, 0.005 g of $[IL]_2[PdBr_4]$ was added and heated for 10, 30, 60, or 180 min, respectively. After that time, the solvent was removed under reduced pressure. The residue was dissolved in $CHCl_3$, filtered, and used for analysis.

Samples containing the reaction substrates (boronic acid or aryl halide) were only filtered before analysis.

All MS and tandem MS experiments were performed on a Bruker Daltonics micrOTOF-Q. The ions were generated from electrospray ionization source. The electrospray flow rate was 10 $\mu l/min^{-1}$, which was maintained by a syringe pump; the spray was directed into a heated glass capillary at a temperature of 200 °C and a high voltage of 4500 V between the endplate and the spray needle. Nebulizer vacuum: 0.4 Bar; dry gas flow: 4.0 l/min.

4.5. Crystallographic data collection and refinement

Single crystal of $[mioe]_2[PdCl_4]$ suitable for X-ray measurements was selected for the diffraction data collection. Crystal was mounted on glass fibers in silicone grease, cooled to 100 K in a nitrogen gas stream, and the diffraction data was collected on a Kuma KM-4 CCD diffractometer with graphite monochromated Mo Kα radiation (λ = 0.71073 Å). The structure was subsequently solved using direct methods and developed by full least-squares refinement on F^2. Structural solution and refinement was carried out using SHELX suite of programs [29]. Analytical absorption corrections (performed with CrysAlis RED [30]) were applied for compound. C, N, O, Cl, and Pd atoms were refined anisotropically. The carbon-bonded H atoms were positioned geometrically and refined isotropically using a riding model. Crystal data and structure refinement are summarized in Table 6. The molecular structure plots (Fig. 2) were prepared using the ORTEP-3 program [31].

The molecules of $[mioe]_2[PdCl_4]$ are linked by numerous weak hydrogen interactions (Table 7) of C–H···Cl and C–H···O type [17]. As a consequence, a three-dimensional network of such interactions is formed in the crystal. Even though some of the listed H···Cl distances may at first appear to be fairly long compared to the expected values, the presence of C-H···Cl hydrogen bonds was confirmed spectroscopically for tetrachloropalladate complexes with H···Cl spacings even above 3 Å [9].

4.6. Suzuki–Miyaura reaction procedure

The S–M reaction was carried out in a 50 cm^3 Schlenk tube. The solid substrates: base (1.2 mmol) and phenylboronic acid (1.1 mmol, 0.134 g) were weighted and placed in the Schlenk tube. Next, 3 cm^3 of the solvent, and 2-bromotoluene (1 mmol, 0.118 cm^3) were added with an automatic pipette. After heating the substrates to the

required temperature (40 °C), the palladium complex (0.01 mmol, 0.0059 g) was added. The reactor was closed with a rubber plug, and the reaction mixture was stirred in 40 °C. After the given reaction time, the reactor was cooled down and the organic products were extracted with 10 cm^3 of *n*-hexane (5 min with stirring). Next, 2 cm^3 of water was added to the organic layer, 5 cm^3 of the upper *n*-hexane layer was taken, and 0.038 cm^3 of dodecane was added as an internal standard. The organic products were analyzed using the GC–MS method (instrument HP 5890 II with capillary column ELITE-5MS and stationary phase 5% diphenylpolysiloxane, 95% dimethylpolysiloxane).

Acknowledgements

The authors thank Marek Hojniak, MSc (Faculty of Chemistry, University of Wrocław) for performing the GC–MS analyses.

Financial support from grant PBZ-KBN-118/T09/2004 is gratefully acknowledged.

References

[1] J.E.L. Dullius, P.A.Z. Suarez, S. Einloft, R.F. De Souza, J. Dupont, Organometallics 17 (1998) 815.
[2] S. Bouquillon, A. du Moulinet d'Hardemare, M. Averbuch-Pouchot, F. Henin, J. Muzart, Polyhedron 18 (1999) 3511.
[3] I. Pryjomska-Ray, A.M. Trzeciak, J.J. Ziółkowski, J. Mol. Catal. A: Chem. 257 (2006) 3.
[4] I. Pryjomska-Ray, A. Gniewek, A.M. Trzeciak, J.J. Ziółkowski, W. Tylus, Top. Catal. 40 (2006) 1.
[5] C. Kuan Lee, H. Han Peng, I.J.B. Lin, Chem. Mater. 16 (2004) 530.
[6] M.F. Ortwerth, M.J. Wyzlic, R.G. Baughman, Acta Cryst. C54 (1998) 1594.
[7] C.J. Adams, P.C. Crawford, A.G. Orpen, T.J. Podesta, B. Salt, Chem. Commun. (2005) 2457.
[8] C. Zhong, Y. Zuo, H. Jin, T. Wang, S. Liu, Acta Cryst. E62 (2006) m2281.
[9] W. Zawartka, A. Gniewek, A.M. Trzeciak, Ł. Drzewiński, T. Lis, Acta Cryst. E62 (2006) m1100.
[10] W. Zawartka, A.M. Trzeciak, J.J. Ziółkowski, T. Lis, Z. Ciunik, J. Pernak, Adv. Synth. Catal. 348 (2006) 1689.
[11] C.W.K. Gstöttmayr, V.P.W. Böhm, E. Herdtweck, M. Grosche, W.A. Herrmann, Angew. Chem. Int. Ed. 41 (2002) 1364.
[12] G. Altenhoff, R. Goddard, C.W. Lehmann, F. Glorius, Angew. Chem. Int. Ed. 42 (2003) 3690.
[13] R.B. Bedford, C.S.J. Cazin, D. Holder, Coord. Chem. Rev. 248 (2004) 2283.
[14] A. Tudose, A. Maj, X. Sauvage, L. Delaude, A. Demonceau, A.F. Noels, J. Mol. Catal. A: Chem. 257 (2006) 158.
[15] X. Yang, Z. Fei, T.J. Geldbach, A.D. Phillips, C.G. Hartinger, Y. Li, P.J. Dyson, Organometallics 27 (2008) 3971.
[16] J.G. De Vries, Dalton Trans. (2006) 421.
[17] O. Navarro, R.A. Kelly III, S.P. Nolan, J. Am. Chem. Soc. 125 (2003) 16194.
[18] M.B.A. Song, Org. Lett. 3 (2001) 3761.
[19] M.T. Reetz, E. Westermann, Angew. Chem. Int. Ed. 39 (2000) 165.
[20] M. Moreno-Manas, R. Pleixats, S. Villarroya, Organometallics 20 (2001) 4524.
[21] S. Bhattacharya, A. Srivastava, S. Sengupta, Tetrahedron Lett. 46 (2005) 3557.
[22] A. Gniewek, J.J. Ziółkowski, A.M. Trzeciak, M. Zawadzki, H. Grabowska, J. Wrzyszcz, J. Catal. 254 (2008) 121.
[23] M.A. Aramendia, F. Lafont, M. Moreno-Manas, R. Pleixats, A. Roglands, J. Org. Chem. 64 (1999) 3592.
[24] A.A. Sabino, A.H.L. Machado, C.R.D. Correia, M.N. Eberlin, Angew. Chem. Int. Ed. 43 (2004) 2514.
[25] P.-A. Enquist, P. Nilsson, P. Sjöberg, M. Larhed, J. Org. Chem. 71 (2006) 8779.
[26] H. Guo, R. Qian, Y. Liao, S. Ma, Y. Guo, J. Am. Chem. Soc. 127 (2005) 13060.
[27] L.S. Santos, G.B. Rosso, R.A. Pilli, M.N. Eberlin, J. Org. Chem. 72 (2007) 5809.
[28] F.A. Cotton, Inorg. Synth. XIII (1972) 52.
[29] G.M. Sheldrick, SHELXS-97 and SHELXL-97, University of Göttingen, Germany, 1997.
[30] Oxford Diffraction, CrysAlis RED Version 1.171.31.5, Oxford Diffraction Ltd., Wrocław, Poland, 2005.
[31] L.J. Farrugia, J. Appl. Crystallogr. 30 (1997) 565.